Journal of Photochemistry and Photobiology A: Chemistry 204 (2009) 144–147

Contents lists available at ScienceDirect

Journal of Photochemistry and Photobiology A: Chemistry

journal homepage: www.elsevier.com/locate/jphotochem

Improvement of electron transport by low-temperature chemically assisted sintering in dye-sensitized solar cell

Kyungkon Kim, Gi-Won Lee, Kicheon Yoo, Dong Young Kim, Jun-Kyung Kim, Nam-Gyu Park*

Materials Science and Technology Division, Korea Institute of Science and Technology (KIST), 39-1 Hawolgok-dong, Seongbuk-gu, Seoul 136-791, Republic of Korea

ARTICLE INFO

Article history:
Received 21 February 2008
Received in revised form 16 January 2009
Accepted 16 March 2009
Available online 24 March 2009

Keywords:
Dye-sensitized solar cell
Interparticle connection
Low-temperature coating
Chemically assisted sintering

ABSTRACT

We have succeeded in preparing TiO_2 film at low-temperature using a binder-free paste and a process of low-temperature crystallization of anatase formed from hydrolysis of $TiCl_4$ at 150 °C. The electron diffusion coefficient of the chemically assisted sintered dye-sensitized solar cell (DSSC) was 3 times larger at the 1×10^{17} photons flux than that of non-sintered one. This is thought to be ascribed from the formation of inter-connecting TiO_2 between the TiO_2 nanoparticles by chemically assisted sintering process.

1. Introduction

Since discovery of low-cost and high-efficiency dye-sensitized solar cells (DSSCs) based on nanocrystalline TiO_2 [1], researches on DSSCs have been progressed remarkably. DSSC is typically fabricated with a dye-adsorbed mesoporous TiO_2 film on transparent conductive substrate, an iodide–iodine redox electrolyte and a platinum-coated counter electrode. Light absorbed dye molecules generate electrons and holes which are separated by electron-injection into TiO_2 and hole-transfer to redox electrolyte. Nanoparticle interconnection in the mesoporous TiO_2 layer serves as pathway for photo-injected electrons. Among the components comprising DSSC, nanoparticulate TiO_2 film is primarily of importance because its surface area and interparticle connectivity have influence on photovoltaic performance, associated with amount of dye adsorption and electron transport.

Recently low-temperature fabrication methods of DSSCs have been attracted much attention since they offer advantages over conventional high-temperature methods, such as light-weight and flexible DSSC application. Moreover, low-temperature processible technique may be beneficial to fabrication of multilayer structure with different dyes, similar to tandem solar cells based on compound semiconductors [2], which can enhance solar energy conversion efficiency because of utilizing spectrum splitting. In DSSC, mesoporous TiO_2 films are conventionally prepared by coating a binder-contained viscous TiO_2 paste on a transparent conductive substrate, followed by heating it at temperature around 500 °C to mainly sinter the TiO_2 nanoparticles. The sintered nanoparticles could provide a good electrical pathway for transporting photo-injected electrons. In this regard, the most important step toward low-temperature DSSC fabrication lies in how to induce nanoparticle interconnection at a temperature lower than the thermal sintering condition. Several methods have been proposed to fabricate TiO_2 film at low-temperature by using spin-coating [3], compression [4–7], electrophoretic [8–10], electron beam curing [11], and hydrothermal techniques [12]. Among the proposed methods, physical compression method improved the conversion efficiency compared with electrophoretic and electron beam curing methods, in which the compressed film with thickness of 8 μm demonstrated 5.3% at a reduced light intensity of 0.1 sun (10 mW/cm^2) [7]. However, the efficiency decreased significantly to 2.5% at higher light intensity of 1 sun condition (100 mW/cm^2). This indicates that the interparticle connection was incomplete by the physical compression method. A steam-treatment of a deposited film, composed of nanocrystalline TiO_2 and titanium salt, in autoclave was proposed, where 18 μm-thick TiO_2 films showed conversion efficiencies of about 4% along with good linearity of photocurrent with light intensity [12]. However a further high-temperature post-treatment of the low-temperature steamed film improved the maximum incident photon-to-current conversion efficiency (IPCE) from 41% to 88%, indicating that electrical contact is still inferior compared with thermal sintered TiO_2 film. Recently, a layer transfer method was proposed, where the TiO_2 film deposited on a removable substrate was first annealed at 450 °C, removed from the substrate, transferred to the second substrate, and finally compressed [13]. The film prepared by a layer transfer

* Corresponding author. Tel.: +82 2 958 5365; fax: +82 2 958 5309.
E-mail address: npark@kist.re.kr (N.-G. Park).

1010-6030/$ – see front matter © 2009 Elsevier B.V. All rights reserved.
doi:10.1016/j.jphotochem.2009.03.008

method showed relatively high efficiency compared with the other reported methods due to the fact that it was sintered first at high-temperature and then compressed at low-temperature. Although the layer transfer method can exhibit high efficiency, it still takes an advantage of high-temperature thermal sintering process.

Previously, we reported a low-temperature method to fabricate TiO_2 layer by using newly developed binder-free TiO_2 paste with high viscosity of 5×10^4 cP [14]. The binder-free paste-derived film dried at 150 °C demonstrated conversion efficiency at 1 sun light intensity of 2.5% for the ~4 μm-thick transparent film and ~3.5% for the same film with additional light scattering layer. We have tried to improve further interparticle connection and eventually found an effective route to inter-connect TiO_2 nanoparticles without taking advantage of thermal sintering and/or compression processes. Here we report an effective sintering route to prepare a low-temperature processible dye-sensitized solar cell, where it is found that the conversion efficiency of a non-thermally sintered TiO_2 film is comparable to that of the cell prepared by high-temperature thermal sintering method.

2. Experimental

Binder-free TiO_2 paste was first prepared according to the procedure reported previously [14], where the binder-free TiO_2 paste was prepared by adding 63 mg of 10 M ammonia solution to 10 g of 12.5 wt.% acidic TiO_2 colloid solution for 1 h. The binder-free TiO_2 paste was spread onto a transparent conducting glass substrate (Pilkington, TEC8) by the doctor-blade technique at ambient temperature and dried at 150 °C for 15 min. The dried film was cooled down to ambient temperature and then immersed in 0.2 M $TiCl_4$ solution for 10 min at 4 °C. The $TiCl_4$-treated film was blown by nitrogen gas for a few seconds to remove the $TiCl_4$ solution from the surface of the film, which was immediately transferred to the hot plate that was pre-heated to 150 °C and kept for 15 min (hereafter this film will be denoted as "*chemically assisted sintered film* (CS film)"). It is thought that the $TiCl_4$ solution that was inside pores of mesoporous TiO_2 will be remained even after quick N_2 blowing and changed to TiO_2 during the chemically assisted sintering process. The thickness of the CS film was about 4.0 ± 0.2 μm. For the comparison, we prepared a TiO_2 film by simply drying the binder-free TiO_2 paste at 150 °C (*non-sintered film* (NS film)). We also prepared high-temperature (450 °C) sintered TiO_2 films that were made from the binder-free (TS film) and the binder containing (TSB film) paste. The resulting film was immersed in absolute ethanol containing 5×10^{-4} M of N 719 dye (commercial name is 535-bisTBA, Solaronix SA) for 24 h at room temperature. Solar cells based on those films were prepared according to the method described elsewhere [15]. The redox electrolyte consisted of 0.6 M 1,2-dimethyl-3-hexyl-imidazolium iodide (C6DMII), 0.2 M LiI, 40 mM I_2 and 0.5 M 4-*tert*-butylpyridine in acetonitrile/valeronitrile (50:50, v/v%) was used. The solar cells prepared from the NS film, CS film, TS film and TSB film will be denoted as cell NS, cell CS, cell TS and cell TSB, respectively.

For transient photocurrent studies, the cells were probed with a weak laser pulse at 532 nm superimposed on a relatively large, background (bias) illumination at 680 nm with a setup similar to the reported one [18]. The bias light was illuminated by a 0.5 W diode laser (B&W TEK Inc., Model: BWF1-670-300E/55370). Neutral density filters were used to adjust the intensity of the bias light. A 30 mW frequency-doubled Nd:YAG laser (Laser-Export Co. Ltd. Model: LCS-DTL-314QT) (λ = 532 nm, pulse duration 10 ns) was used as probe light to estimate the transient time. The current transient data were obtained by using a Stanford Research Systems model SR570 low-noise current preamplifier, amplified by a Stanford Research Systems model SR560 low-noise preamplifier, and recorded on a Tektronix TDS 3054B 500 MHz oscilloscope. The photocurrent induced by the probe light was adjusted to have less than 1% intensity than that induced by the bias light.

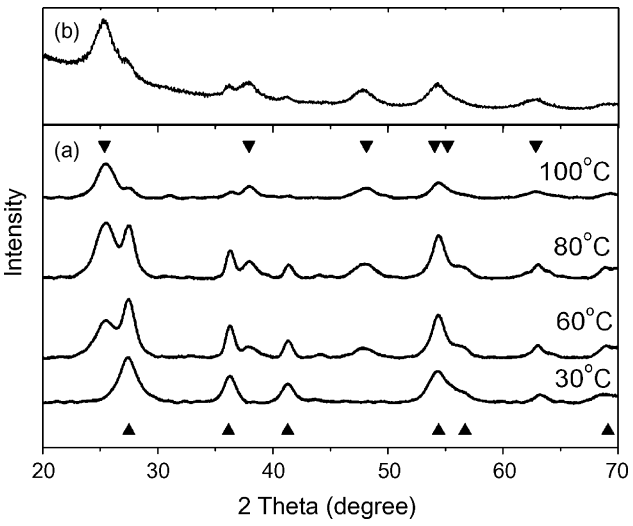

Fig. 1. (a) XRD spectrum of the TiO_2 formed from the $TiCl_4$ solution with the different hydrolysis temperature and (b) XRD spectra of the TiO_2 thin layer prepared by annealing the 0.2 M $TiCl_4$ thin layer on FTO glass. Down and up triangles represent peak position of anatase and rutile TiO_2, respectively.

3. Results and discussion

The binder-free paste was hydrolyzed in the $TiCl_4$ solution to improve the interparticle connection between TiO_2 nanoparticles. Since the binder-free TiO_2 paste film consists of anatase phase TiO_2 nanoparticles and the electron diffusion coefficient of the anatase TiO_2 is one-order of magnitude larger than that of the rutile one [16], it is desirable if TiO_2 nanoparticles are inter-connected by the anatase TiO_2. However, we observed that the rutile phase TiO_2 was formed by room temperature hydrolysis of $TiCl_4$ in the previous studies [17].

Because the TiO_2 nanoparticle has anatase phase and, furthermore, very thin layer would be formed on the TiO_2 nanoparticles after hydrolysis of $TiCl_4$, it is difficult to determine the proper temperature for the formation of anatase phased inter-connecting TiO_2 by XRD. However, it could be found by an alternative way. We traced the change of the crystalline phase of TiO_2 by changing the hydrolysis temperature of the $TiCl_4$ solution. As shown in the XRD spectrum (Fig. 1(a)), the crystalline structure of the TiO_2 depends on the hydrolysis temperature. The rutile phase was dominantly formed when $TiCl_4$ solution is hydrolyzed at the 30 °C. A mixture phase of rutile and anatase was observed from the hydrolysis temperature of 60 °C. The anatase phase became dominant above the hydrolysis temperature of 100 °C. Based on the XRD spectra, we decided to conduct CS process at the 150 °C. We hydrolyzed the $TiCl_4$ solution on the FTO glass at the hydrolysis temperature of 150 °C and the XRD spectrum of the obtained TiO_2 is shown in Fig. 1(b). The XRD spectrum suggests that the thin film of $TiCl_4$ layer on the FTO glass was converted to anatase phase TiO_2 layer after annealing at 150 °C. If we consider that the thickness of TiO_2 nanoparticle layer (~4 μm) is negligible to the thickness of the FTO glass (2 mm), it is thought that the thermal conduction to the thin layer of $TiCl_4$ should be similar without concerning the existence of TiO_2 layer on the FTO glass. As a result, we can expect that the $TiCl_4$ embedded in the TiO_2 film is mostly converted to anatase phase after 150 °C hydrolysis.

Fig. 2 and Table 1 compare the photovoltaic performance of cell NS, cell CS, cell TS and cell TSB. The efficiency of the cell CS was enhanced up to 47% compared with cell NS. From the cell CS-to-cell

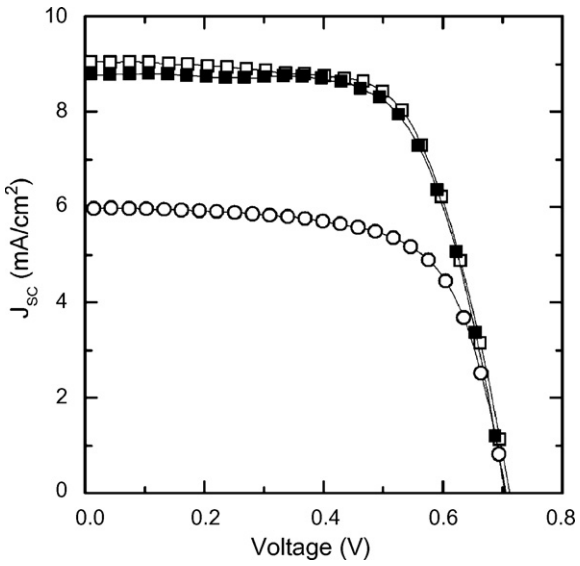

Fig. 2. Comparison of photocurrent–voltage curves of dye-sensitized solar cells prepared by non-sintered (cell NS; open circle), chemically sintered (cell CS; solid square), and 450 °C thermally sintered (cell TS; open square) TiO_2 nanoparticle layer.

Table 1
Photovoltaic properties of dye-sensitized solar cells.

		Thickness (μm)	J_{SC} (mA/cm^2)	V_{OC} (V)	Fill factor (%)	Efficiency (%)
Binder-free	Cell NS	4.2	5.96	0.706	67.2	2.83
	Cell	4.0	8.77	0.704	67.6	4.18
	CS	8.0	8.55	0.649	69.5	3.85
	Cell	4.1	8.37	0.776	73.2	4.76
	TS	7.4	9.71	0.773	71.4	5.36
Binder	Cell	4.7	9.03	0.712	66.3	4.27
	TSB	8.5	13.1	0.712	66.6	6.21

NS ratio of J_{SC}, V_{OC} and FF, it seems that the efficiency enhancement was mainly ascribed to increased J_{SC} rather than FF and V_{OC}.

We supposed such an enhancement could be derived from the better interparticle connection between TiO_2 particles. It is expected that improved interparticle connection resulted in longer electron diffusion length (or shorter electron transport) time and longer recombination time of the cell. In order to investigate the effect of chemically assisted sintering on the diffusion length and recombination time of DSSC, we have conducted the photocurrent and photovoltage transient measurement on the non-sintered (cell NS) and chemically sintered (cell CS) DSSC.

Usually, time constant for the transient of injected electrons in the nanocrystalline TiO_2 (nc-TiO_2) films is in the millisecond domain, which is several order of magnitude slower than that of single crystalline TiO_2 and it is related to the traps of TiO_2 nanoparticles [19]. As a result, the transient time and diffusion coefficient (D) of the electrons in the nc-TiO_2 strongly depends upon the trap density of the nc-TiO_2 films. The distribution of trap density is related to the photoexcitation density of the films. It is well known that the D value increases as the light intensity increases. Therefore, the D value has to be estimated for the different photoexcitation or photocarrier density [20,21].

Since, the absorption coefficient of dye used in our experiment is low enough (ca. 500 cm^{-1}) at the bias light wavelength (680 nm), we expect that the bias light provides homogeneous photocarrier density throughout the nc-TiO_2 films in the cell [19]. In this experiment, bias laser excites dyes and generates uniform photocurrent and the change of the photocurrent generated by the probe laser pulse was recorded by time. The data was obtained with different bias light intensity and the time constant was obtained by fitting a decay of the photocurrent transient with $\exp(-t/\tau_C)$, where t is time.

At photocurrent transient measurement, the time constant for electron collection is related to the electron diffusion coefficient (D) by the expression [19]

$$D = \frac{d^2}{2.35\tau_C} \quad (1)$$

where d is the film thickness and τ_C is a time constant.

The obtained diffusion coefficient of cell CS and cell NS are shown in Fig. 3(a). As shown in Fig. 3(a), the diffusion coefficient of the cell CS is significantly larger than that of the cell NS without concerning the bias light intensity. Furthermore, the difference became larger as the bias light intensity increases.

The charge recombination time (τ_R) could be obtained in a similar way. We recorded the decay of photovoltage by time and fitted the decay curve with single exponential decay function ($\exp(-t/\tau_R)$). Fig. 3(b) compares charge recombination time that obtained from the photovoltage transient measurement of the cells. The charge recombination time of the cell CS is longer than that of cell NS. We can expect that the charge collection efficiency of the cell CS is higher than that of cell NS due to longer diffusion length and recombination time. This clearly shows that the electron transport in cell CS was significantly improved compared to that in cell NS after chemically assisted sintering process.

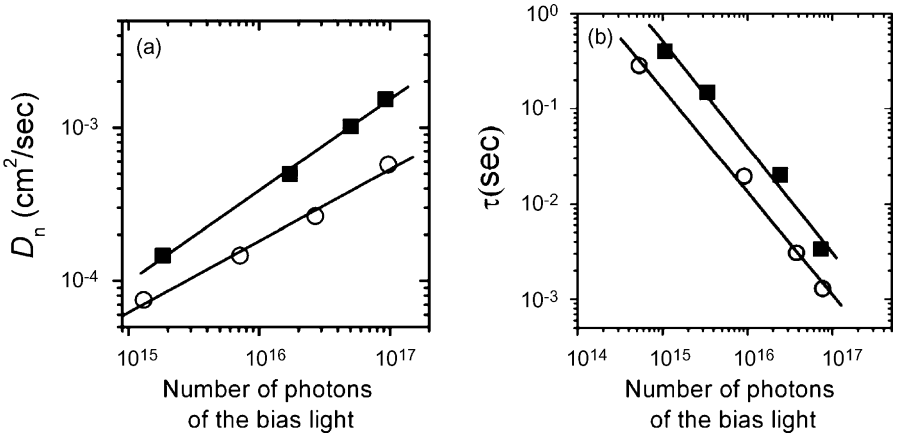

Fig. 3. (a) Electron diffusion coefficients and (b) recombination lifetime of electrons for the cell NS (open circle) and cell CS (solid square) obtained by photocurrent transient measurement and photovoltage transient, respectively.

Several groups reported efficiency improvement by the $TiCl_4$ treatment on the thermally sintered TiO_2 electrode [22,23]. Some of them claimed that $TiCl_4$ treatment enhances dye absorption and improves charge injection due to the shift in conduction band edge of the TiO_2 nanoparticles rather than improvement of carrier transport in TiO_2 film [23]. It is thought that the electron transport of thermally sintered TiO_2 film is sufficient even without $TiCl_4$ treatment because TiO_2 nanoparticles are interconnected during the high-temperature sintering. In case of chemically assisted sintering, $TiCl_4$ treatment could help the interconnection between the nanoparticles because it is not enough to inter-connect the TiO_2 nanoparticles only by the low-temperature (150 °C).

Although the improvement of electron transport is thought to play an important role for the efficiency enhancement of the cell CS, the dye absorption enhancement and electron-injection improvement also could play a role on the enhanced performance of the cell.

As shown in Fig. 2 and Table 1, the efficiency of the chemically assisted sintered solar cell (cell CS) was comparable to the solar cell having similar thickness of thermally sintered TiO_2 layer (cell TSB). However, the efficiency of the cell CS was lower than the cell TSB when the TiO_2 layer was increased to 8 μm (Table 1). This could be attributed to the porosity difference between chemically and thermally sintered TiO_2 films. It is known that a binder polymer is used to control the pore size of the porous TiO_2 film. The binder polymer is burned during the high-temperature sintering process to develop pores in the TiO_2 film. Benkstein et al., controlled the porosity of the TiO_2 film by changing the binder polymer-to-TiO_2 ratio [24]. The porosity of the TiO_2 film was increased as the binder polymer content increased and the lowest porosity was obtained from the binder-free paste. Also, Kijitori et al., used binder-free paste of 60 nm TiO_2 nanoparticle for the non-sintered TiO_2 film to have a similar porosity as the TiO_2 films prepared from the sintering of 20 nm binder containing paste [25]. We can expect chemically assisted sintering method will not accommodate development of nanopore structure compared with binder containing TiO_2 paste. To exclude the influence of binder in the paste, we prepared a TiO_2 film by thermal sintering of the binder-free paste at the temperature of 450 °C (cell TS). As shown in Table 1, the efficiency of the cell TS film was also comparable with cell CS and cell TSB at the 4 μm TiO_2 film thickness. However, the efficiency of the cell TS became lower than that of cell TSB at the thickness of 8 μm. Since both films are sintered at the high enough temperature, it is expected that the nanoparticles are inter-connected successfully. Only possible structural difference between the two films is the pore size. This result also supports that the inferior nanopore development in chemically sintered TiO_2 layer could limit the electrolyte mass transport as the layer thickness increase. The J_{SC} of the cell prepared with the thermally sintered binder containing TiO_2 paste (cell TSB) was increased up to 45% as the film thickness was increased. Whereas, there was only 16% increase in J_{SC} for the cell prepared with the thermally sintered binder-free TiO_2 paste (cell TSB). This is ascribed to the porosity difference as we described in the text.

For the cell CS, there was slight decrease in J_{SC} with increase of the TiO_2 film thickness. It is thought that there is an additional effect on the J_{SC} reduction besides reduced porosity of the TiO_2 film. The particle interconnection by the chemically assisted sintering (CS) will not perfect as the thermal sintering. This imperfect connection should be considered for the J_{SC} decrease as well as lower porosity. The electron transport between particles inter-connected with CS method seems to work at the relatively thin TiO_2 film (4.0 μm). However, the transport could be limited at the thicker film (8.0 μm), which resulted in the lowering charge collection efficiency (J_{SC}).

4. Conclusions

In conclusion, we have succeeded in preparing TiO_2 film at low-temperature using a binder-free paste and a process of low-temperature crystallization of anatase formed from hydrolysis of $TiCl_4$ at 150 °C. The resulting film exhibits comparable conversion efficiency to the high-temperature thermally sintered film. The formation of thin layer of anatase phase by chemically assisted sintering method at low-temperature connects well with the nanocrystalline TiO_2 particles, resulting in good electrical contact for transporting photoinjected electrons.

Acknowledgements

This work was supported in part by the Korea Institute of Science and Technology (KIST) Institutional Programs (2E20750), and the Ministry of Education, Science and Technology (MEST) Research Programs under the contract number of 2N31000.

References

[1] B. O'Regan, M. Grätzel, Nature 353 (1991) 737.
[2] J.M. Olson, D.J. Friedman, S. Kurtz, Handbook of Photovoltaic Science and Engineering, 1st ed., John Wiley & Sons Ltd., England, 2002.
[3] F. Pichot, J.R. Pitts, B.A. Gregg, Langmuir 216 (2000) 5626.
[4] H. Lindström, A. Holmberg, E. Magnusson, S.-E. Lindquist, L. Malmqvist, A. Hagfeldt, Nano Lett. 1 (2001) 97.
[5] H. Lindström, A. Holmberg, E. Magnusson, L. Malmquist, A. Hagfeldt, J. Photochem. Photobiol. A 145 (2001) 107.
[6] G. Boschloo, H. Lindström, E. Magnusson, A. Holmberg, A. Hagfeldt, J. Photochem. Photobiol. A 148 (2002) 11.
[7] S.A. Haque, E. Palomares, H.M. Upadhyaya, L. Otley, R.J. Potter, A.B. Holmes, J.R. Durrant, Chem. Commun. 24 (2003) 3008.
[8] J.-H. Yum, S.-S. Kim, D.-Y. Kim, Y.-E. Sung, J. Photochem. Photobiol. A: Chem. 173 (2005) 1.
[9] T. Miyasaka, Y. Kijitori, J. Electrochem. Soc. 151 (2004) A1767.
[10] D. Matthews, A. Kay, M. Grätzel, Aust. J. Chem. 47 (1994) 1869.
[11] T. Kado, M. Yamaguchi, Y. Yamada, S. Hayase, Chem. Lett. 32 (2003) 1056.
[12] D. Zhang, T. Yoshida, H. Minoura, Adv. Mater. 15 (2003) 814.
[13] M. Dürr, A. Schmid, M. Obermaier, S. Rosselli, A. Yasuda, G. Nelles, Nat. Mater. 4 (2005) 607.
[14] N.-G. Park, K.M. Kim, M.G. Kang, K.S. Ryu, S.H. Chang, Y.-J. Shin, Adv. Mater. 17 (2005) 2349.
[15] N.-G. Park, M.G. Kang, K.S. Ryu, K.M. Kim, S.H. Chang, J. Photochem. Photobiol. A: Chem. 161 (2004) 105.
[16] S. Kambe, S. Nakade, Y. Wada, T. Kitamura, S. Yanagida, J. Mater. Chem. 12 (2002) 723.
[17] N.-G. Park, G. Schlichthorl, J. van de Lagemaat, H.M. Cheong, A. Mascarenhas, A.J. Frank, J. Phys. Chem. B 103 (1999) 3308.
[18] N. Kopidakis, K.D. Benkstein, J. van de Lagemaat, A.J. Frank, J. Phys. Chem. B 107 (2003) 11307.
[19] J. Van de Lagemaat, A.J. Frank, J. Phys. Chem. B 105 (2001) 11194.
[20] N. Kopidakis, E.A. Schiff, N.-G. Park, J. van de Lagemaat, A.J. Frank, J. Phys. Chem. B 104 (2000) 3930.
[21] S. Nakade, Y. Saito, W. Kubo, T. Kitamura, Y. Wada, S. Yanagida, J. Phys. Chem. B 107 (2003) 8607.
[22] S. Ito, P. Liska, P. Comte, R. Charvet, P. Pechy, U. Bach, L. Schmidt-Mende, S.M. Zakeeruddin, A. Kay, M.K. Nazeeruddin, M. Grätzel, Chem. Commun. (2005) 4351.
[23] P.M. Sommeling, B.C. Oregan, R.R. Haswell, H.J.P. Smit, N.J. Bakker, J.J.T. Smits, J.M. Kroon, J.A.M. Van Roosmalen, J. Phys. Chem. B 110 (2006) 19191.
[24] K.D. Benkstein, N. Kopidakis, J. van de Lagemaat, A.J. Frank, J. Phys. Chem. B 107 (2003) 7759.
[25] Y. Kijitori, M. Ikegami, T. Miyasaka, Chem. Lett. 36 (2007) 190.